Concentrations of dissolved dimethyl sulphide (DMS), methanethiol and other trace gases in context of microbial communities from the temperate Atlantic to the Arctic Ocean

Valérie Gros[1], Bernard Bonsang[1], Roland Sarda-Estève[1], Anna Nikolopoulos[2], Katja Metfies[3], Matthias Wietz[3,4] and Ilka Peeken[3]

[1] Laboratoire des Sciences du Climat et de l'Environnement, CNRS-CEA-UVSQ, IPSL, Gif sur Yvette, 91 191, France
[2] Norwegian Polar Institute, Fram Centre, 9296 Tromsø, Norway
[3] Alfred Wegener Institute Helmholtz Centre for Polar and Marine Research, 27570 Bremerhaven, Germany
[4] Max Planck Institute for Marine Microbiology, 28359 Bremen, Germany

Correspondence to: Valérie Gros (valerie.gros@lsce.ipsl.fr)

Abstract.

Dimethyl sulphide (DMS) plays an important role in the atmosphere by influencing the formation of aerosols and cloud condensation nuclei. In contrast, the role of methanethiol (MeSH) for the budget and flux of reduced sulphur remains poorly understood. In the present study, we quantified DMS and MeSH together with the trace gases carbon monoxide (CO), isoprene, acetone, acetaldehyde and acetonitrile in North Atlantic and Arctic Ocean surface waters, covering a transect from 57.2°N to 80.9°N in high spatial resolution. Whereas isoprene, acetone, acetaldehyde and acetonitrile concentrations decreased northwards, CO, DMS and MeSH retained significant concentrations at high latitudes, indicating specific sources in polar waters. DMS was the only compound with higher average in polar (31.2 ± 9.3 nM) than in Atlantic waters (13.5 ± 2 nM), presumably due to DMS originating from sea ice. At eight sea-ice stations north of 80°N, in the diatom-dominated marginal ice zone, vertical profiles showed a marked correlation (R^2 = 0.93) between DMS and chlorophyll a. Contrary to previous measurements, MeSH and DMS did not co-vary, indicating decoupled processes of production and conversion. The contribution of MeSH to the sulphur budget (represented by DMS+MeSH) was on average 20% (and up to 50%) higher than previously observed in the Atlantic and Pacific Oceans, suggesting MeSH as a significant source of sulphur possibly emitted to the atmosphere. The potential importance of MeSH was underlined by several correlations with bacterial taxa, including typical phytoplankton associates from the *Rhodobacteraceae* and *Flavobacteriaceae* families. Furthermore, the correlation of isoprene and chlorophyll a with *Alcanivorax* indicated a specific relationship with isoprene-producing phytoplankton.

Overall, the demonstrated latitudinal and vertical patterns contribute to understanding how concentrations of central marine trace gases are linked with chemical, and biological parameters across oceanic waters.

1 Introduction

Volatile Organic Compounds (VOCs) and carbon monoxide (CO) are important in atmospheric chemistry as precursors of ozone and secondary organic aerosols, which affect air quality and climate. The oceans become increasingly considered as sources and sinks of CO and VOCs with potential influence on atmospheric chemistry, despite being globally a small source compared to anthropogenic emissions (Duncan et al., 2007; Kansal, 2009) and terrestrial vegetation (Guenther et al., 1995). Biological activities substantially contribute to the dynamics of short-lived VOCs like dimethyl sulphide (DMS) and isoprene. For instance, dimethylsulfoniopropionate (DMSP) produced by phytoplankton and other marine organisms(such as macro-algae, corals and sponges, Jackson and Gabric, 2022 and references therein) can be metabolized by bacteria into DMS. DMS is rapidly oxidized once emitted to the atmosphere (mean lifetime of 1 day), then representing a major precursor of sulphate aerosols with radiative impacts by scattering sunlight and constituting condensation nuclei (CCN), with a potential cooling impact on climate (through the change in clouds microphysics). The role of DMS emissions on climate has been first hypothesized by Shaw, (1983) and Charlson et al., (1987) and is known as the CLAW hypothesis, which has been largely discussed and debated since then. A very extensive literature exists on the link between DMSP and DMS on the one hand and on the multi-steps of the oxidation of DMS to sulphate and corresponding impact on CCN on the other hand. As both processes are beyond the scope of this paper, we refer the reader to the recent review of (Jackson and Gabric, 2022 and references therein) for further information. Alternatively, DMSP can be microbially demethylated into methanethiol (CH_3SH, herein referred to as MeSH) (Kiene, 1996; Kiene and Linn, 2000), whose role in the atmosphere and oceans is poorly characterized to date (Lawson et al., 2020). The oxidation of MeSH by hydroxyl radicals OH (Tyndall and Ravishankara, 1991; Butkovskaya and Setser, 1999) effectively produces SO_2, with up to 48% based on model calculations (Novak et al., 2022). Thus, MeSH is probably an underestimated factor in the marine gaseous sulphur cycle.

Isoprene, another important trace gas, can be produced by photosynthesizing organisms over short timescales (a few hours), with potential influence on regional atmospheric chemistry and aerosol formation above biologically active pelagic waters (Bikkina et al., 2014). Photosynthetic cyanobacteria are stronger emitters of isoprene than diatoms, with taxon-specific variability in production (Bonsang et al., 2010; Shaw et al., 2010). Besides direct emission by primary producers, oceanic trace gases can originate from photochemical processes. For instance, isoprene can be also photochemically produced at the sea-surface microlayer (Ciuraru et al., 2015). In addition, photodegradation of dissolved organic matter is the main source of CO (Wilson et al., 1970), although laboratory experiments showed a minor contribution of biological activities (Gros et al., 2009).

The oceanic contribution to the budget of oxygenated VOCs (OVOC) is also important to consider, since OVOCs may affect the oxidative capacity of the remote atmosphere through the budget of tropospheric radicals (Singh, 2004). A recent study has confirmed the importance of air-sea exchange for acetaldehyde, pointing out the lack of oceanic measurements (Wang et al., 2019). Marine waters can be either local source or sink of OVOCs depending on the region. Acetone and acetaldehyde are considered to originate from photodegradation of dissolved organic carbon (Zhou and Mopper, 1997; Zhu and Kieber, 2019).

A positive net flux of acetone is generally observed in biologically productive areas such as tropical upwelling zones, whereas sink are located at high latitudes or in oligotrophic waters (Lawson et al., 2020). As OVOCs mainly originate from terrestrial sources, their air-sea fluxes can also be a net deposition, when their marine atmospheric concentrations are directly influenced by air masses originating from continents (Phillips et al., 2021). Furthermore, the OVOCs acetone, methanol, acetonitrile and acetaldehyde can show seasonal variation (Davie-Martin et al., 2020).

Linking the dynamics of (O)VOCs and trace gases to primary production and microbial distribution helps understanding fundamental couplings between biological, oceanic and atmospheric processes. This is particularly important in the Arctic Ocean, which warms two to three times faster than the global average (Schmale et al., 2021 and references therein). These processes concur with changing physical, biological and photochemical variability, subsequently affecting the coupling between ocean and atmosphere. Importantly, sea-ice melt influences VOCs production, e.g. through increased primary production in ice-free waters (Arrigo and van Dijken, 2015), release of ice algae and their substrates (Fernández-Méndez et al., 2014), as well as higher gas exchange at the ocean-atmosphere interface (Lannuzel et al., 2020) when ice-free areas expand. This impact of sea-ice has been shown to DMSP, DMS, isoprene, acetone and acetaldehyde in the Canadian Arctic (Galindo et al., 2014; Wohl et al., 2022; Galí et al., 2021). Concurrent changes in phytoplankton distribution can amplify these dynamics, for instance via the northward expansion of the coccolithophorid *Emiliania huxleyi* by Atlantic currents (Hegseth and Sundfjord, 2008; Oziel et al., 2020) and changing bloom phenologies (Nöthig et al., 2015; von Appen et al., 2021). As phytoplankton and bacterial distribution are often linked, these dynamics subsequently affect the heterotrophic food web. The bacterial families *Rhodobacteraceae* and *Flavobacteriaceae* are frequently abundant during phytoplankton blooms, contributing to the degradation of algal organic matter and the conversion of DMSP into DMS and MeSH (Moran et al., 2012; Moran and Durham, 2019). Campen et al., (2022) have recently emphasized the need to better link bacterial distribution with DMS and CO metabolism. In addition, the production and degradation of e.g. isoprene might be an important, yet understudied contribution to biogeochemical cycles (Carrión et al., 2020; Rodríguez-Ros et al., 2020).

Contextualizing marine VOCs, trace gases and microbes in Arctic vs temperate Atlantic waters is important, as Atlantic characteristics expand northward with climate change (Polyakov et al., 2020). Here, we report concentrations of DMS, MeSH, isoprene, CO, acetone, acetaldehyde and acetonitrile in context of microbial distribution across the North Atlantic and Arctic Oceans. During the TRANSSIZ campaign on-board RV Polarstern from early spring to summer 2015, we continuously measured these compounds in surface waters between 57° to 80°N, and additionally over vertical profiles from the surface to 50 m depth in the ice-covered region north of Svalbard (Fig. 1). The main objective was to document the concentrations and spatial variability of trace gases, specifically the ratio between MeSH and DMS, in context of phytoplankton numbers, bacterial diversity and water masses. To our knowledge, this is the first survey of MeSH in the Arctic Ocean, shedding light on its biogeochemical role in an area of rapid climate change.

2 Material and methods

2.1 Campaign description and oceanographic parameters

Water samples were collected during the TRANSSIZ ("Transitions in the Arctic Seasonal Sea Ice Zone"; PS 92 - ARK XXIX/1) cruise on-board RV Polarstern between May 19th and June 28th, 2015. The cruise started in Bremerhaven, Germany, and ended in Longyearbyen, Svalbard (Fig. 1), as described in detail by Peeken (2016).

Along the ship track between May 19th and 27th, trace gases were continuously measured in the surface water layer. Salinity, temperature and chlorophyll a (Chl a) fluorescence were continuously measured with the FerryBox System of the Helmholtz-Zentrum Geesthacht (HZG) in surface water (6 m depth). The instrument performs a self-cleaning routine every day with acid washing and freshwater rinsing. In addition, sensor behavior is controlled by staff members of Polarstern and usually no drift of the sensors is observed (for details see Petersen (2014)). Temperature, salinity and Chl a were extracted from the database every 2 minutes. The sensor for Chl a was a submersible fluorometer (Turner Designs, Sunnyvale, CA, USA) with excitation/emission wavelengths of 325 nm and 425 nm respectively.

After May 27th, eight ice stations (number 19, 27, 31, 32, 39, 43, 46, and 47, Table S1) were carried out over the continental shelf north of Svalbard and over the Yermak Plateau (Fig. 1; Table S1). At each ice station, the ship was anchored to an ice floe at drift for approximately 36 h. While carrying out ice work on the port side, winch-operated instruments were deployed in the open water on the starboard side to record biological and biogeochemical variables including trace gases and phytoplankton pigments. Except for the first ice station (in 70% ice cover and still some leads present), the stations were conducted in almost 100% ice cover (Massicotte et al., 2019) with the sampling taking place in small leads. All ice stations were 50 to 250 km away from the ice edge and open water (Dybwad et al., 2021). A detailed study of nutrients, marker pigments and protist microscopy classified the Yermak Plateau stations (39, 43, 46) to be in a pre-bloom phase, while all other stations were in a bloom phase (Dybwad et al., 2021). During the ice stations, discrete seawater samples for trace gas and phytoplankton composition analysis were collected at six different depths of the water column using the CTD (conductivity, temperature, depth) water-sampling carousel. These samples were collected in 1 L light-proof flasks for direct analysis on board. Values for temperature and salinity were provided by the CTD bottle data file for each station (Nikolopoulos et al., 2016).

Temperature and salinity from both types of sampling were used to classify the sampled water masses based on the criteria applied in Tran et al., 2013 (Table1).

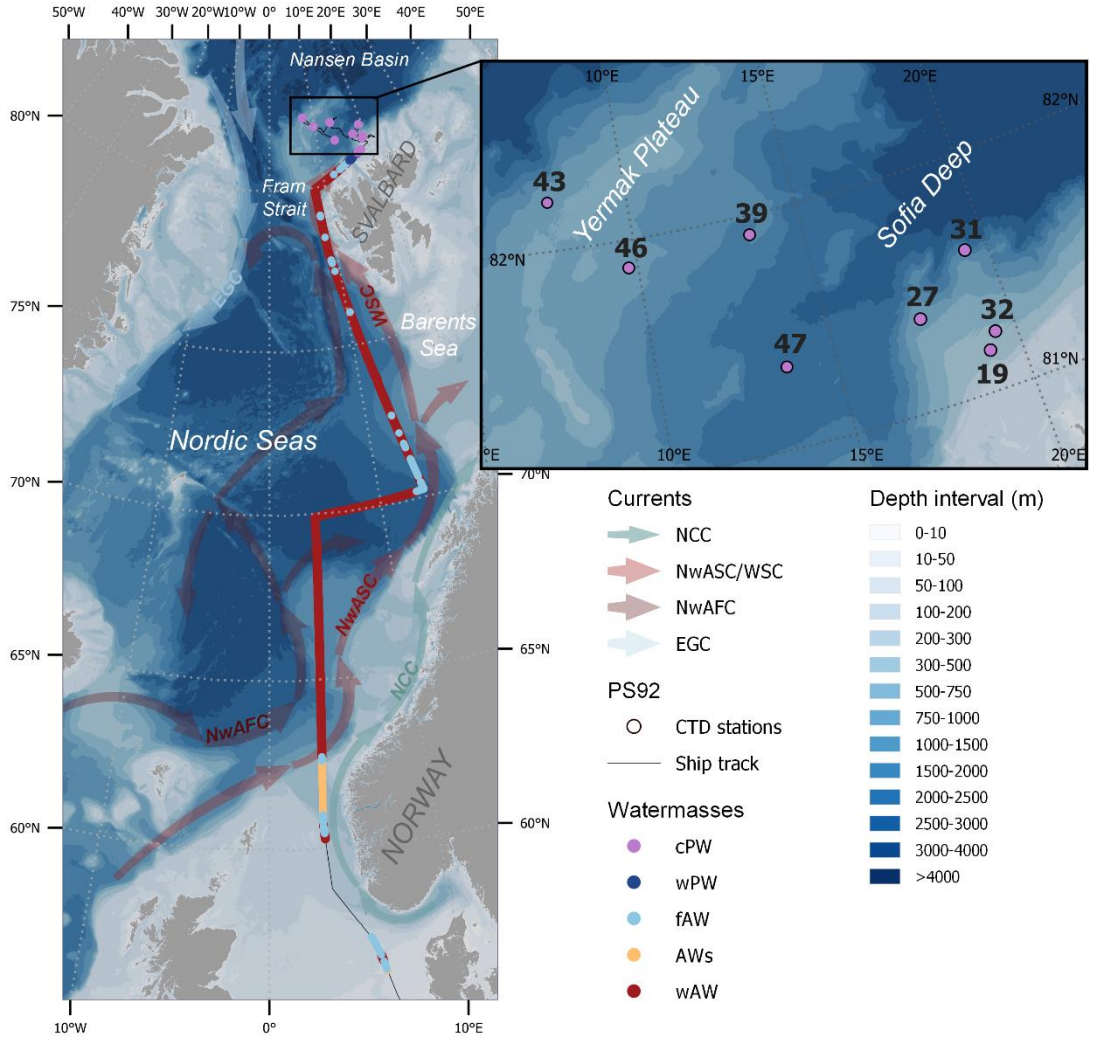

Fig. 1: Ship track colored by water mass: 'regular' warm Atlantic Water (wAW), coastal influenced Atlantic water with low salinity (AWs), freshened and cooled Atlantic Water (fAW), warm Polar Water (wPW) and cold Polar Water (wPW), determined according to the temperature and salinity criteria in Table 1. Surface measurements were sampled continuously between 57°N and 81°N, and vertical profiles were sampled at eight sea ice stations (black insert and Table S1). The background map shows the bathymetry by GEBCO Compilation Group (GEBCO Bathymetric Compilation Group 2022, 2022) and a schematic overview of the major currents influencing the surface waters in the study area, as adopted from Skagseth et al. (2022): the Norwegian Atlantic Slope Current (NwASC), West Spitsbergen Current (WSC), Norwegian Atlantic Front Current (NwAFC), Norwegian Coastal Current (NCC) and East Greenland Current (EGC).

2.2 Biological measurements

2.2.1 Pigment analysis

For pigment analysis with high pressure liquid chromatography (HPLC), seawater samples (1–2 L) were taken from Niskin bottles mounted on a CTD rosette from six depths in the upper 50 m (Table S1). All samples were analysed within few hours after collection.

Sample handling and pigment measurements were carried out as described in Tran et al. (2013). The FerryBox/surface Chl a data were calibrated against surface Chl a concentrations derived from Niskin bottles ($R^2 = 0.83$, see Fig. S1). The taxonomic composition of phytoplankton was calculated from marker pigments using the CHEMTAX approach (for details see Wollenburg et al., (2018)), distinguishing diatoms, *Phaeocystis*-type haptophytes, prasinophytes, chlorophytes, dinoflagellates, cryptophytes, chrysophytes and coccolithophorid-type haptophytes. The contribution of each group was expressed as Chl a concentrations.

2.2.2 Bacterial community analysis

In total 34 seawater samples for bacterial community analysis were collected along the transect (Table S2) at a depth of ~10 m using the AUTOFIM system (Metfies et al., 2016, 2020), which is installed at the bow of RV Polarstern next to the ship's pump system intake. Per sampling event, two liters of seawater were filtered onto polycarbonate filters with 45 mm diameter and 0.4 µm pore size (Millipore; USA) at 200 mbar. Filters were stored at -80°C until DNA extraction in the home laboratory using the NucleoSpin Plant II kit (Macherey-Nagel, Germany) according to the manufacturer's instructions. Bacterial 16S rRNA gene fragments were amplified using primers 515F–926R (Parada et al., 2016) according to the 16S Metagenomic Sequencing Library Preparation protocol (Illumina, San Diego, CA). Amplicon gene libraries were sequenced using Illumina MiSeq technology in 2x300 bp paired-end runs at CeBiTec (Bielefeld, Germany). Raw sequence files have been deposited in the European Nucleotide Archive under accession number PRJEB50492, using the data brokerage service of the German Federation for Biological Data (GFBio) in compliance with MIxS standards. The complete amplicon analysis workflow is described in Supplement S2, with Rscripts documented under https://github.com/matthiaswietz/transsiz. Briefly, after primer removal using cutadapt (Martin, 2011), reads were classified into amplicon sequence variants (ASVs) using DADA2 (Callahan et al., 2016) and taxonomically classified using the Silva v138 database (Quast et al., 2012). We obtained on average 85,000 quality-controlled, chimera-filtered reads per sample (Table S2) sufficiently covering community composition (Fig. S2). Nonmetric multidimensional scaling was performed to determine bacterial community variability along the transect. Associations between the abundance of bacterial ASVs and environmental parameters were determined via Holm-corrected Spearman's correlations. Only correlations >|0.4| were considered, and only if higher than with latitude to omit indirect signals due to geographical variability.

2.3 Trace gas measurements

Carbon monoxide and VOCs dissolved in seawater were measured in real-time along the transect using samples from the Ferrybox water intake (6 m depth). Seawater was delivered by the ship membrane pump to the laboratory for continuous injection into an online water extraction device (OLWED; Supplement S3, Fig. S3). Furthermore, we measured trace gas concentrations from the surface (0.5 m) to 50 m depth at the eight ice stations, analysing all samples within few hours after collection. Possible causes of artefacts during this storage period have been investigated in a previous experiment in the same area (Tran et al., 2013), showing no significant losses of low molecular weight VOCs and a slow decrease for CO during the first 4 hours (Xie and Zafiriou, 2009 and Tolli and Taylor, 2005).

2.3.1 PTRMS measurements

VOC were quantified using a high sensitivity Proton-Transfer Mass Spectrometer (PTRMS, Ionicon Analytik) developed by Lindinger and Jordan (1998) and since then widely used (see for example review by Blake et al., (2009)). The measurement principle of PTRMS is based on the soft chemical ionization of VOCs by proton-transfer. This proton-transfer reaction is possible for all compounds having a proton affinity higher than the one from water, giving access to a large variety of VOCs (Blake et al., 2009). During the campaign, air from the headspace was continuously sampled by the PTRMS through a ⅛ inch PFA line at a flowrate of about 60 ml/min using usual parameters, i.e. 60°C (inlet and drift tube temperature), 600V drift tube and 2.2 mbar drift tube pressure (with a corresponding E/N of 132 Td, towsend). The estimated residence time of about 30 seconds should prevent any degradation or adsorption of the extracted gases in the system. Furthermore, a series of standards were measured under the same experimental conditions, showing high linearity in the system's response. This observation supports the absence of artefacts in the experimental procedure. Measurements were usually performed every 2.5 minutes, except for every 10 min for about 24h (between 61.1 °N to 65.3°N), when they were only performed every 10 min in order to scan a wider range of masses (m/z) and to select the compounds of interest, i.e. showing a signal above the detection limit. After this, about 25 masses (m/z) were selected to be further monitored (with dwell times from 1 to 20 s). Here, we present the results for the compounds with the most significant variability, i.e. isoprene, dimethyl sulphide, methanethiol, acetone, acetaldehyde, and acetonitrile. The only small fragmentation from soft ionization allow direct measurements of compounds at their corresponding m/z+1. Although we cannot rule out higher molecule fragment on the measured m/z+1, interferences from other compounds are likely negligible for the masses presented in this manuscript (Blake et al., 2009; Yuan et al., 2017). An exception could be isoprene, as it can contain fragmentation of 2-methyl-3-buten-2-ol (MBO) or of cyclohexanes. However, during the period when the PTRMS measured in scan mode, MBO mass (m/z 87) has shown no correlation (R^2= 0,02) with m/z 69. In addition, the good correlation (R^2= 0.77) between isoprene and Chl a across vertical profiles (see Figure S7) confirms that the measured m/z 69 can be mainly attributed to isoprene. For acetone, the signal corresponds to “acetone + propanal” but propanal can be neglected and m/z 59 be considered as acetone (de Gouw and Warneke, 2007). The PTRMS used for this campaign had been used the year before on a field campaign and some of its characteristics are described elsewhere (Zannoni

et al., 2016). The calibration procedures (in the gas and water phases) are given in Supplement S4, Figures S4a and S4b. The measurement uncertainty with this PTRMS had been estimated at ± 20% taking into account errors on standard gas, calibrations, blanks, reproductibility / repetability and linearity (Baudic et al., 2016). The overall uncertainty for dissolved VOC measurements was estimated at ± 30%.

205

2.3.2 CO measurements

CO was measured using a custom-made gas chromatograph directly coupled to the extraction cell and equipped with a hot mercuric-oxide detector operating at 265°C (RGA3, Trace Analytical, Menlo Park, CA, USA). The system comprised two 1-mL nominal volume stainless-steel injection loops (for samples and calibration, respectively), previously calibrated in the
210 laboratory. The chromatographic procedure used a pre-column (0.77m length, 0.32 cm outer diameter, containing Unibeads 1S 60/80 mesh) and an analytical column (0.77m length, 0.32 cm outer diameter, containing molecular Sieve 13X 60/80 mesh) both heated to 95°C. Air sample (from the headspace of the extraction cell) and standard gas were alternately injected into the chromatograph, each sample being directly calibrated with the previous injection of the standard gas. The standard gas consisted of CO diluted in synthetic air at a nominal concentration of 200 ppbv. The CO retention time was 1.5 min, and a
215 complete chromatogram ran for 2.5 min. The overall accuracy of the measurement was about 5%. More details about CO measurements can be found in Gros et al. (1999) and Tran et al. (2013).

3 Results

3.1 Latitudinal variability in surface waters from 57°N to 80°N

220 Along the latitudinal transect, we performed online surface measurements of Chl a and hydrographic parameters, covering five different water masses: warm Atlantic Water with low salinity (AWs), 'regular' warm Atlantic Water (wAW), freshened and cooled Atlantic Water (fAW), cold Polar Water (cPW) and warm Polar Water (wPW) as defined in Table 1 following Tran et al. (2013). The major part of the transect, from 63 to 80°N, occurred in wAW (Fig. 1). Fresher (low-saline) Atlantic Water (AWs and fAW) was encountered in the vicinity of the Norwegian Coastal Current (NCC) which carries water masses
225 influenced by river run-off: AWs at 60.6-62.3 °N (with fAW in the mixing zones), and fAW around 70-72°N. Fresher mixed products (fAW) were also intermittently encountered west of Svalbard (where AW meets fjord/coastal water masses), as well as in the marginal ice zone where AW mixes with and gradually subducts under fPW. Polar Water (PW) only occurred north of 80°N in the Nansen Basin. Surface temperature steadily decreased northwards, from 8°C to below 0°C in the ice-covered region >80°N (Fig. 2). The slight deviation around 70°N corresponds to the shifting cruise track towards Tromsø due to a
230 medical evacuation event (cf. Fig. 1). Chl a concentrations peaked at the beginning of the transect, with overall five areas

where concentrations exceeded 1 µg L^{-1} indicating increased phytoplankton abundances: ~ 60°N to 61°N (up to 2 µg L^{-1}), several locations >66°N (>6-8 µg L^{-1}), and three additional peaks (>5 µg L^{-1}) at 76°, 78°, and 79.5°N, respectively. Within the marginal ice zone (>80°N) Chl a concentrations reached up to 3 µg L^{-1}.

3.1.1 Trace gas distribution

The oxygenated gases acetone and acetaldehyde strongly decreased with higher latitudes and lower water temperatures, being below or close to the detection limit >70°N. Nevertheless, we observed a 2- to 3-fold increase between 61°N and 65°N. Acetone varied from 20 to 25 nM between 57 to 65°N, decreasing to 0.1 nM near 80°N. A maximum of 40 nM between 60°N and 65°N covaried with higher Chl a concentrations, plus a second minor peak between 77°N and 79°N. Similar latitudinal trends occurred for acetaldehyde and acetonitrile. Acetaldehyde decreased from 15 nM in the temperate Atlantic to 0.5-3 nM in the Arctic Ocean, with a peak of approx. 40 nM between 60°-65°N. Acetonitrile decreased from 1.5 nM to 0.1-0.5 nM, with a second maximum of approx. 2 nM between 60° and 65°N. Isoprene decreased from 4-5 pM at 57°N to 0.3-1.5 pM at 80°N, with three additional maxima along the transect. Opposed to the other trace gases, isoprene slightly increased again north of 80°N, albeit at a much lower concentration compared to lower latitudes.

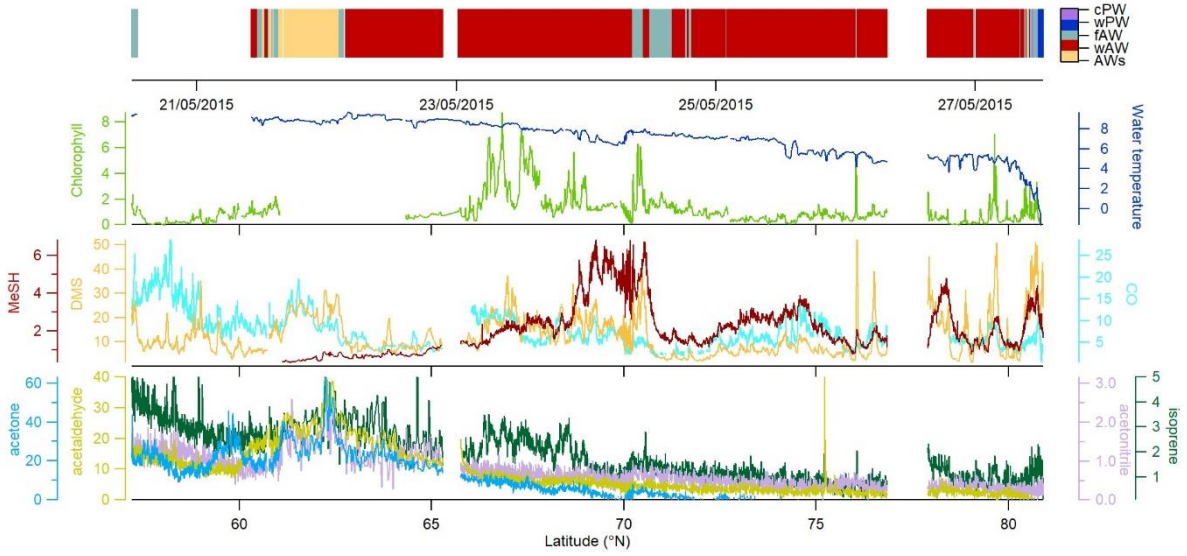

Fig. 2: Latitudinal variability of acetone (nM), acetaldehyde (nM), acetonitrile (nM), isoprene (pM), DMS (nM), MeSH (nM), and CO (nM) between 57.2°N to 80.9°N in relation to Chl a (µg L^{-1}) and water temperature (°C). Due to sensor failure temperature values are missing until ~61°N. On the top panel, the colored horizontal bar represents the different encountered water masses (Fig. 1). Values below 3 nM are below the detection limit for acetone and acetaldehyde, see S4.

CO, DMS and MeSH displayed different patterns, retaining high but variable concentrations at high latitudes. CO concentrations varied between 2 and 30 nM, with several peaks covarying with Chl a at 62.5, 67 and 77.6°N. DMS ranged from ~2 nM to 50 nM, with peaks occurring at 61-63°N, 66-70.5°N and a maximum of 60 nM at 80°N. MeSH varied from 0.1 to 7 nM, with concentration peaks near 70°N and between 73-75°N.

255

3.1.2 Bacterial communities in the environmental context

We performed 16S rRNA amplicon sequencing to characterize bacterial community structure in context of latitude, water temperature and trace gas concentrations. Correspondent to the known microbial differences between temperate and polar oceans (Sunagawa et al., 2015), communities substantially varied by latitude and temperature (Fig. 3). These factors explained
260 43% of bacterial variability (PERMANOVA; $p < 0.001$). Several correlations between trace gases, Chl a and the abundance of specific ASVs (Fig. 3) suggests bacterial linkages with phytoplankton and VOC dynamics. Correlations were both positive and negative, sometimes differing within single genera. For instance, one SAR92-ASV positively correlated with MeSH, whereas another SAR92-ASV negatively correlated with DMS. For MeSH and its ratio to DMS, correlations differed between *Pseudofulvibacter*, NS10, OM75, *Yoonia-Loktanella* and *Ascidiaceihabitans* ASVs (negative) versus SUP05 (positive).
265 Interestingly, we detected negative correlations of *Synechococcus* and an unclassified cyanobacterial ASV with MeSH. DMS positively correlated with ASVs from *Aurantivirga* and SAR11 clade Ia. Two ASVs from the NS9 clade were unique in their correlations with acetone and acetonitrile. Furthermore, several ASVs from *Thalassolituus* and *Alcanivorax* (negative), NS5 and *Polaribacter* (positive) correlated with Chl a and isoprene.

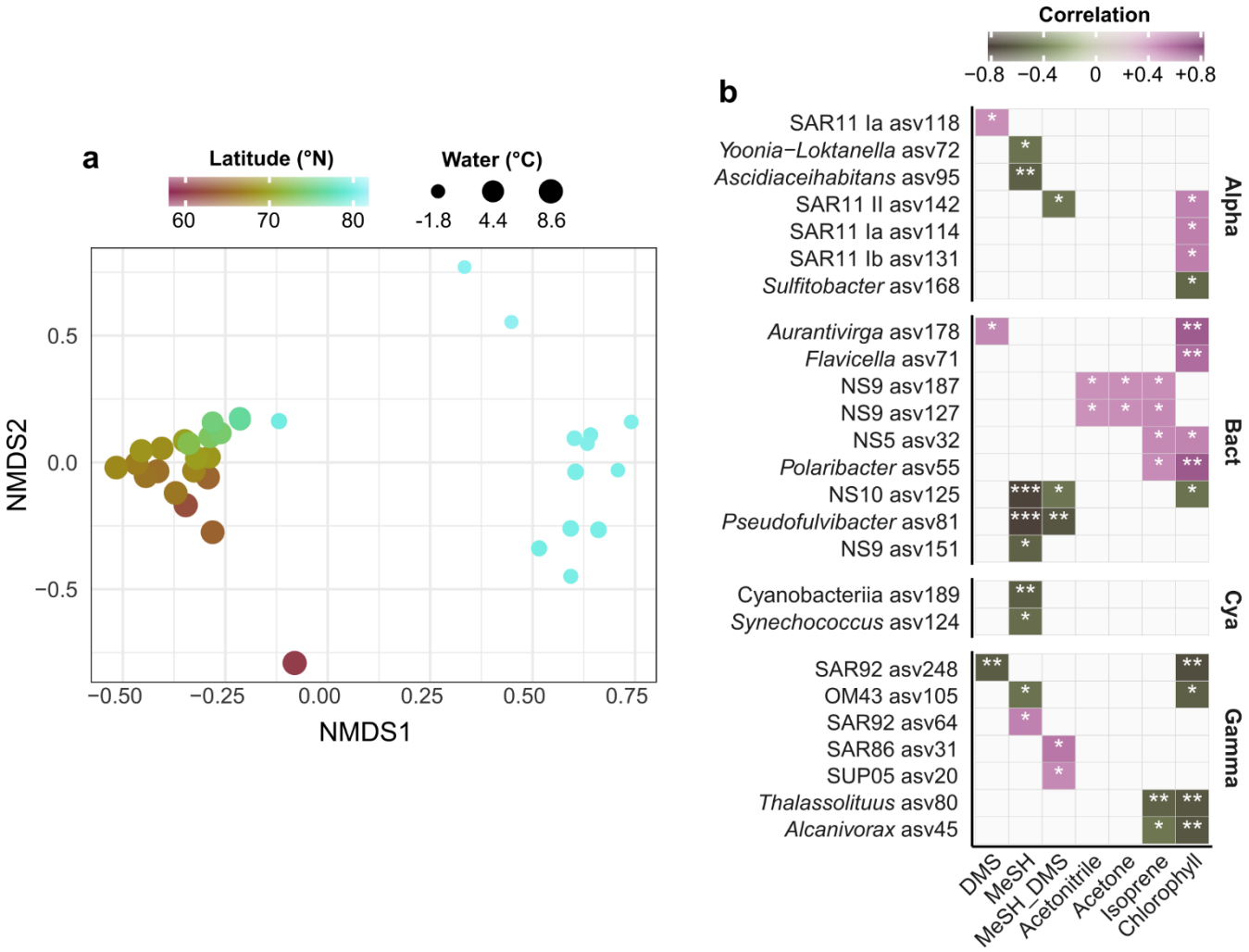

Fig. 3. a) Nonmetric multidimensional scaling of bacterial community composition (Bray-Curtis dissimilarities of Hellinger-transformed relative abundances). The colour gradient and dot size illustrate latitude and water temperature respectively. b) Spearman correlations between environmental parameters and the abundance of bacterial ASVs. MeSH_DMS: ratio between MeSH and DMS, expressed as MeSH/(MeSH+DMS). Only correlations >|0.4| are shown, and only if stronger than with latitude. No correlations occurred with acetaldehyde and CO. Alpha: Alphaproteobacteria; Gamma: Gammaproteobacteria; Bact: Bacteroidetes; Cya: Cyanobacteria. Asterisks indicate Holm-corrected p-values (* < 0.05; ** < 0.01; *** < 0.001).

3.2 Vertical under-ice profiles north of 80°N

In the ice-covered region north of Svalbard, we performed vertical under ice profiles at eight stations instead of the continuous surface seawater measurements (Fig. 1, 4, Fig. S5, see section 2.1). To connect the latitudinal and vertical data, we compared the cPW values measured along the transect with the surface values from the vertical profiles (Tab. 1, Fig. 4). This revealed

marked differences in trace gas concentrations compared to the polar water masses along the transect, except for acetonitrile. Acetaldehyde concentrations (0.3 to 14.2 nM with an average of 7.2 ± 4.4 nM for surface values, i.e. 0.5 m under water) were much higher than in polar waters in the northern part of the transect (0.8 ± 2.0 nM) and more in the range of the previously described wAW (4.8 ± 4.0 nM) and fAW (9.8 ±5.6 nM). A similar increase was apparent for acetone, with values closer to wAW than to polar waters. DMS varied substantially (from 1.6 to 31.9 nM for the surface values) at the sea-ice stations. DMS concentrations at the bloom stations 19 and 32 (see section 2.1 and Fig. 4) were in the range of the previously described transect polar waters, whereas the pre-bloom stations (39, 43, 46) only showed >2 nM DMS for surface values. MeSH and CO both exhibited lower concentrations (0.13 ± 0.17 nM and 1.45 ± 1.67 nM respectively) at the sea-ice stations. In contrast, isoprene concentrations were higher (3.2 ±2.1 pM) at the sea-ice stations compared to all other water masses along the transect. The substantial difference between polar waters observed in the northern part of the transect and surface waters from sea-ice stations was also evident in Chl a, marker pigments of relevant phytoplankton groups (diatoms and *Phaeocystis*), and some trace gases (DMS, MeSH, CO, isoprene). The shallow shelf stations 19 and 32 featured a marked phytoplankton bloom with up to 10 µg L^{-1} of Chl a, with diatoms constituting 90% of phytoplankton, indicative of a typical spring bloom scenario (Degerlund and Eilertsen, 2010). Station 27, 31 and 47 had roughly 50% diatom contribution while the pre-bloom stations 39, 43 and 46, were characterized by low biomass (Chl a < 0.5 µg L^{-1}) and a mixed pico- and nanophytoplankton community including prasinophytes, chlorophytes, dinoflagellates, cryptophytes, chrysophytes and coccolithophorid-type haptophytes (Fig. S5).. *Phaeocystis*, a typical bloom-forming organism in the high Arctic (Degerlund and Eilertsen, 2010) constituted up to 80% of phytoplankton biomass at station 47, but their contributions was much lower compared to *Phaeocystis* under-ice bloom in the same region and year reported by (Assmy et al., 2017). This indicates a declining bloom during our sampling period towards the end of June. Except for the Yermak plateau stations (39, 43, 46), *Phaeocystis* contributed between 10-40% of the phytoplankton biomass.

We observed a strong correlation between DMS and Chl a (R^2 Pearson's correlation coefficient = 0.93; Fig. S6). Since diatoms were the most prominent photosynthetic group at ice-covered stations (Fig. 4) we consider them important for DMS fluxes in the Polar Ocean.

Isoprene also markedly correlated with Chl a (R^2 = 0.6, Fig. S6), but only when excluding station 19. This correlation supports a biological source of isoprene, in line with the shown linkage of isoprene and Chl a maxima (Tran et al., 2013). Station 19 was the only station where diatoms almost exclusively dominated the phytoplankton biomass. As shown in laboratory experiments, cold-water diatoms only emit little isoprene (Bonsang et al., 2010), which could explain the observed pattern.

In contrast to the latitudinal transect, MeSH showed low concentrations at most ice stations, except for station 19 (with higher concentrations and a clear decrease with depth). Station 19 was special since being located above the shelf and harbouring a diatom-dominated phytoplankton community. While the diatom community might also produces MeSH, we have currently no explanation for this specific observation.

Vertical profiles of CO generally decrease with depth (Tran et al., 2013). This supports the notion that CO photoproduction (the main source of CO in the ocean) decreases up to threefold from the surface to 20 m depth (Fichot and Miller, 2010). An

exception is station 31 where CO peaked at 30 m depth. This could indicate the presence of a considerable CO emitter, as the emission of CO can vary by more than an order of magnitude between phytoplankton species (Gros et al., 2009).

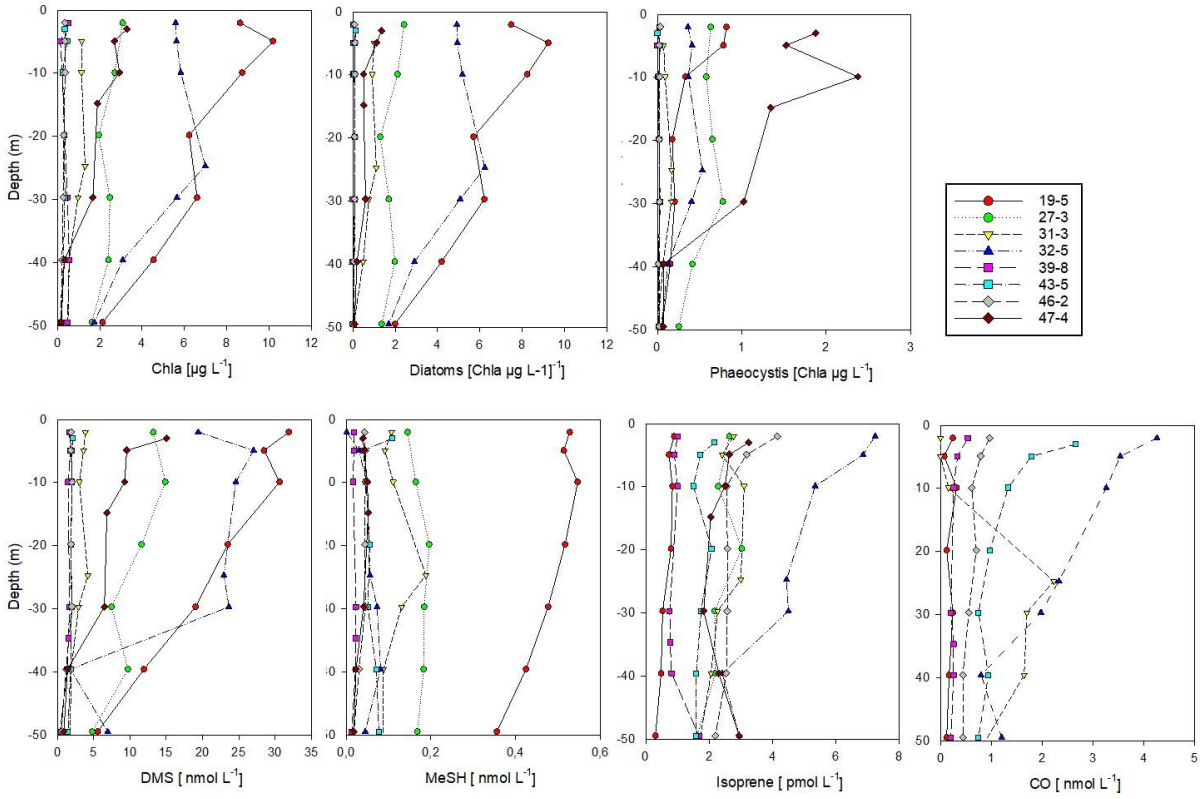

Fig. 4. Vertical profiles of biological parameters and trace gas concentrations's (0-50 m depth) at sea-ice covered stations north of 80°. According to Dybwad et al., (2021) stations 39, 43 and 46 (Yermak Plateau) were in a pre-bloom phase, while all other stations were in a bloom phase. Stations 19 and 32 were shelf stations. The contribution of each phytoplankton group is expressed as Chl a concentrations.

4 Discussion

4.1 Isoprene, CO, acetone, acetaldehyde and acetonitrile

Our study provides a comprehensive overview of biologically and climatically relevant trace gases in the microbiological context; covering ~1400 nautical miles from 57°N to 81°N (May-June 2015) as well as under-ice vertical profiles north of Svalbard. Isoprene and CO can be compared with a previous study (Tran et al., 2013), which was carried out in June-July

2010, i.e. one month later in the summer season and in different water masses (Table 1), but where hardly any phytoplankton blooms were encountered. Concentrations of isoprene, usually associated with phytoplankton (Bonsang et al., 1992; Shaw et al., 2010), were about one order of magnitude lower than described by Tran et al. (2013), even though the biomass indicator Chl a was overall lower (2 µg L^{-1} compared to up to 8 µg L^{-1} reported here). This may relate to seasonal differences in phytoplankton composition, as phytoplankton taxa are known to vary their isoprene emissions (Bonsang et al., 2010; Shaw et al., 2010). Similar seasonal differences in isoprene concentrations were observed by Hackenberg et al., (2017), reporting on average 4.3 pM for March compared to 19.9 pM in July/August in the Arctic sector of the Pacific Ocean. Lower isoprene concentrations in polar waters correspond to values from Ooki et al. (2015), who showed 27 – 33 pM in subpolar and transition waters, and 4 pM in polar waters, respectively. With regard to the vertical profiles, the slight secondary maximum at 20-40 m depth may correspond to the Chl a maximum, as reported by Tran et al. (2013). Nevertheless, the concentrations are overall much lower (about one order of magnitude) than reported by Tran et al., (2013), indicating a high spatial variability of isoprene potentially related to seasonally varying phytoplankton abundances. Simó et al., (2022) recently highlighted the importance of biological consumption of isoprene in water, possibly matching the magnitude of isoprene ventilated to the atmosphere), advising to consider both the sources and sinks when discussing isoprene concentrations and variability. The correlations of *Alcanivorax* and *Thalassolituus* ASVs with both isoprene and Chl a support phytoplankton as source of this trace gas, and subsequent bacterial utilization (Alvarez et al., 2009). In this context, *Alcanivorax* has been reported during phytoplankton blooms in the subarctic Atlantic (Thompson et al., 2020) and can degrade isoprene (Alvarez et al., 2009). *Alcanivorax* and *Thalassolituus* can be associated with microalgal surfaces and also perform hydrocarbon degradation (Love et al., 2021), indicating additional phytoplankton-linked factors that influence their distribution.

Table 1: Mean values and standard deviation for trace gases concentrations in five different water masses along the transect (see Fig. 1 for exact areas), and from surface samples at eight sea-ice stations north of 80°N. S: salinity; BDL: below detection limit. *In italic: data from (Tran et al., 2013) during the ARK XXV expedition in the same area, but in June-July 2010, i.e. one month later in summer. Due to sensor failure of temperature and salinity, the records start at 60°N.

	Acetonitrile (nM)	Acetaldehyde (nM)	Acetone (nM)	DMS (nM)	Methanethiol (nM) MeSH/(MeSH+DMS)	Isoprene (pM)	CO (nM)
Coastal-influenced/low-salinity Atlantic Water (AWs; θ>5°C, S<34.4)	1.11 ± 0.55	19.67 ± 7.96	23.34 ± 12.77	15,65 ± 6.96	0.84 ± 0.65 5.6 ± 7.1	2,55 ± 0.84 *23.4 ± 3.10**	10.70 ± 3.07 *2.50 ± 1.70**
warm Atlantic Water (wAW; θ>2°C, S>34.9)	0.53 ± 0.23	4.84 ± 4.03	2.36 ± 5.88	11,75 ± 6.97	2.89 ± 1.52 21.9 ± 8.7	1,38 ± 0.70 *42.5 ± 49.6**	5.86 ± 2.77 *3.3± 2.2**
freshened Atlantic Water (fAW; θ>1°C, 34.4<S<34.9)	0.94 ± 0.40	9.84 ± 5.60	14.56 ± 10.80	13.05 ± 8.83	3.26 ± 1.49 20.7 ± 10.6	2,66 ± 1.51 *24.8. ± 19.1**	10.17 ± 5.89 *3.4 ± 2.4**
cold Polar Water (cPW; θ<0°C, S<34.7)	0.32 ± 0.13	0.98 ± 2.27	BDL	30.03 ± 9.26	2.80 ± 0.76 9.1 ± 2.3	1,22 ± 0.47	5.00 ± 2.82
warm Polar Water (wPW; θ>0°C, S<34.4)	0.21 ± 0.09	0.30 ± 0.86	BDL	34.65 ± 8.46	3.49 ± 0.29 9.6 ± 2.0	1,06 ± 0.28	7.81 ± 2.08
Polar waters (PW) (cold+warm)	0.30 ± 0.13	0.84 ± 2.05	BDL	31.19 ± 9.29	2.96 ± 0.74 9.2 ± 2.2	1,19 ± 0.44 *14.5 ± 11.5**	5.88 ± 2.91 *6.5 ± 3.2**
Surface water at sea-ice stations > 80°N (range)	0.28±0.12 (0.15-0.47)	7.24±4.43 (0.27-14.23)	2.29±2.79 (0-6.93)	11.22±10.91 (1.64-31.90)	0.13±0.17 (0.02-0.53)	3.23±2.07 (0.90-7.25)	1.45±1.67 (0.24-4.26)

To date, CO in Arctic seawater has only been measured by Tran et al. (2013) in the same Arctic region as well as by Xie and Zafiriou (2009) in the Beaufort Sea. For polar waters, the mean value of 5.9 ± 2.9 nM in surface measurements during the transect matches previously reported averages (6.5 ± 3.2 nM for Tran et al. (2013) and 4.7 ± 2.4 nM for Xie and Zafiriou, (2009) respectively). These concentrations are relatively high compared to the global oceanic mean of 2 nM CO (Conte et al., 2019). Elevated values in the Arctic are not reproduced by the NEMO-PISCES model (Conte et al., 2019), which might be caused by the bio-optical relationship between coloured dissolved organic matter (CDOM) and Chl-a. This model was originally developed for typical oceanic waters (Morel and Gentili, 2009). However, Arctic waters do not conform to this bio-optical type and are considered optically complex waters, with distinct signatures of CDOM and particle loads through the interplay of oceanic, riverine and ice-melt waters (Gonçalves-Araujo et al., 2018). Conte et al., 2019 attribute the release of CO and/or CDOM to sea-ice melt or to lower bacterial consumption in cold waters. The first hypothesis is supported by up to 100 nM CO measured in sea ice (Xie and Gosselin, 2005; Song et al., 2011). . Concerning CO in Atlantic waters, the demonstrated concentrations of up to 10.7 ± 3.1 nM are higher than in polar waters, and exceed data from the same region measured 5 years before (Tran et al., 2013) by up to fourfold. Highest CO values in temperate waters with low Chl a suggest that CO could have originated from an abiotic source, e.g. the photodegradation of CDOM. In vertical under-ice profiles, similar trajectories of Chl a and CO suggest an additional biological source in the euphotic zone, as already shown by Tran et al. (2013). Biological sources of CO have extensively been studied by Gros et al., (2009), and the missing congruency at station 19 might be explained by the relatively low CO emission of cold water diatoms (Gros et al. 2009), since diatoms accounted for the large bloom at our shelf station 19 (Fig. 3).

Considerable differences between Atlantic and polar waters also occurred for acetone, acetonitrile and acetaldehyde. Reference acetone data are scarce (Beale et al., 2013; Tanimoto et al., 2014; Wohl et al., 2020 and references therein), reporting 2 to 40 nM in the temperate and tropical Atlantic (Williams et al., 2004) as well as west Pacific Oceans (Marandino, 2005). In the Atlantic Ocean, (Yang et al., 2014) have observed a mean value of 13.7 nM, without obvious correlation to biological activity. For the Arctic Yang et al., (2014) have reported 6.8 nM in the Labrador Sea and Wohl et al. (2019) 8 ± 2 nM in the Canadian Arctic, matching our data between 65-70°N. Notably, these patterns match the southern Atlantic at 60°S (Wohl et al., 2020), suggesting similar dynamics in both subpolar regions. For acetone, the ocean is considered to be both a photochemical source and a microbial sink depending on the region (Jacob et al., 2002; Fischer et al., 2012). This dual role matches our records of relatively high values for latitudes up to 60°N, and values down to the detection limit in polar zones. For acetonitrile, the oceans are a comparatively small source (originating from phytoplankton) or sink (through bacteria consumption), depending on location and season (see and references therein). The concentrations measured in the present study were mostly >1 nM, and to our knowledge, the first reported in the Arctic Ocean. Overall, little is known about microbial utilization of acetone and acetonitrile, but biogenic effects have been suggested (Davie-Martin et al. (2020). Correlations of NS9 with acetone and acetonitrile indicate an involvement in acetone and acetonitrile cycling among this diverse uncultured clade.

Prior acetaldehyde measurements (Zhou and Mopper, 1997; Kameyama et al., 2010; Yang et al., 2014) reported 1.5 to 5 nM in the North Atlantic Ocean. In the present study, concentrations in AWs (19.7 ± 8.0 nM) were on average twofold higher than those found by Yang et al. (2014) and Zhu and Kieber (2019) in the North Atlantic. However, these related studies measured acetaldehyde in fall, which could explain the difference as the main source of acetaldehyde is attributed to photochemical degradation of CDOM. This corresponds to missing bacterial correlations with this compound.

4.2 DMS and MeSH

Previously reported DMS concentrations in polar oceans varied between 3 to 18 nM (Mungall et al., 2016; Jarníková et al., 2018; Uhlig et al., 2019), with up to 74 nM in the sub-surface Chl a maximum of the Baffin Bay (Galí et al., 2021). Hence, these are overall in the same range as our values. The average around 30 nM observed >80°N might be partly explained by the high DMS concentrations (up to 2000 nM) in sea ice (Levasseur, 2013; see also Hayashida et al., 2020). Indeed, ice-melt derived DMS can contribute up to 50% to the water column inventory (Tison et al., 2010).

Stefels et al. (2007) have suggested no direct relationship between DMS and Chl a on global scale, since the precursor of DMS (DMSP) is produced by diverse phytoplankton at different rates, connected to their physiological state. However, different approaches employed by Gali et al. (2018) and Wang et al. (2020) have shown that Chl a can be a strong predictor of DMS concentrations. In addition, Lana et al., (2012) reported that the DMS-Chl a correlation strongly varies with latitude, with a positive correlation at high latitudes (north of 40°N and south of 40°S). Nevertheless, we note that the figure presented by Lana et al. (2012) shows a lower correlation on the region covered by our transect. The poor correlation found along our transect (R^2 =0.1) probably reflects different phytoplankton types and bloom stages (Dybwad et al., 2021). However, across the vertical under-ice profiles, a strong correlation between Chl a and DMS was found in the Atlantic-influenced polar water masses, mirroring observations by Uhlig et al. (2019). Presumably, this is a typical marginal sea ice zone effect, as found in other sectors of the Arctic (Galí and Simó, 2010; Levasseur, 2013; Park et al., 2013).

Compared to DMS, MeSH has been seldom quantified in marine waters to date, especially at polar latitudes. Leck and Rodhe (1991) have reported on average 0.16 nM MeSH in the Baltic Sea, and 0.28 nM and 0.34 nM in the North Sea respectively. Our data are one order of magnitude higher, ranging from 0.84 ± 0.65 nM in AWs to 3.49 nM in wPW, i.e. in the same range observed by Kiene et al. (2017) in the northeast subarctic Pacific Ocean. These authors have shown that MeSH concentrations in surface waters generally decrease with depth, which overall matches our under-ice vertical profiles (although concentrations were low).

MeSH and DMS originate from the degradation of DMSP, mostly via bacterial demethylation (yielding MeSH) or cleavage (yielding DMS) pathways (Moran and Durham, 2019; Lawson et al., 2020 and references therein). Laboratory experiments have indicated that the net yields of DMS and MeSH from DMSP were on average 32% and 22% respectively (Kiene, 1996). MeSH production might be promoted by low DMSP concentrations and high bacterial sulphur demand (Kilgour et al., 2022).

Mesocosm experiments showed that the proportion of DMS versus MeSH increased from the pre-bloom phase to (induced) bloom conditions (Kilgour et al., 2022). In pelagic waters, DMS generally dominates gaseous sulphur, with MeSH being the second most abundant compound but contributing on average <10% to the total sulphur species in the North and Baltic seas (Leck and Rodhe, 1991), in the Atlantic Ocean (Kettle et al., 2001), and in the Southwest Pacific Ocean (Lawson et al., 2020).

Comparable to some North Sea locations (Leck and Rodhe, 1991), MeSH contributed up to 40% between 70°N-75°N, with a maximum of 50% at 78.6°N (Fig. 5a). This latitudinal variability was underlined by shifts in major bacterial genera. For instance, *Paraglaciecola* (Gammaproteobacteria) and NS4 (Bacteroidetes) peaked together with the *highest* MeSH fraction between 70-80°N. *Amylibacter* decreased towards the north, whereas unclassified *Nitrincolaceae* prevailed >80°N together with an again smaller MeSH/DMS ratio. The overall MeSH contribution of 20% suggests that MeSH represents a considerable fraction of sulphur, with linkages to microbial dynamics. Accordingly, we found several correlations with the abundance of specific ASVs. Correlations between Yoonia-Loktanella and Ascidiaceihabitans ASVs with MeSH reflected the prominent role of Rhodobacteraceae in DMSP demethylation (Curson et al., 2011; Moran et al., 2012). The positive link of SAR11 and SUP05 ASVs corresponds to the prevalence of DMSP-metabolizing genes in these taxa (Nowinski et al., 2019; Landa et al., 2019; Sun et al., 2016). The link between cyanobacteria and MeSH was notable, since DMSP-utilizing genes have been rarely found in cyanobacteria (Liu et al., 2018). Hence, there might be indirect effects on other photosynthetic organisms, indicating yet undescribed chemical linkages among primary producers.

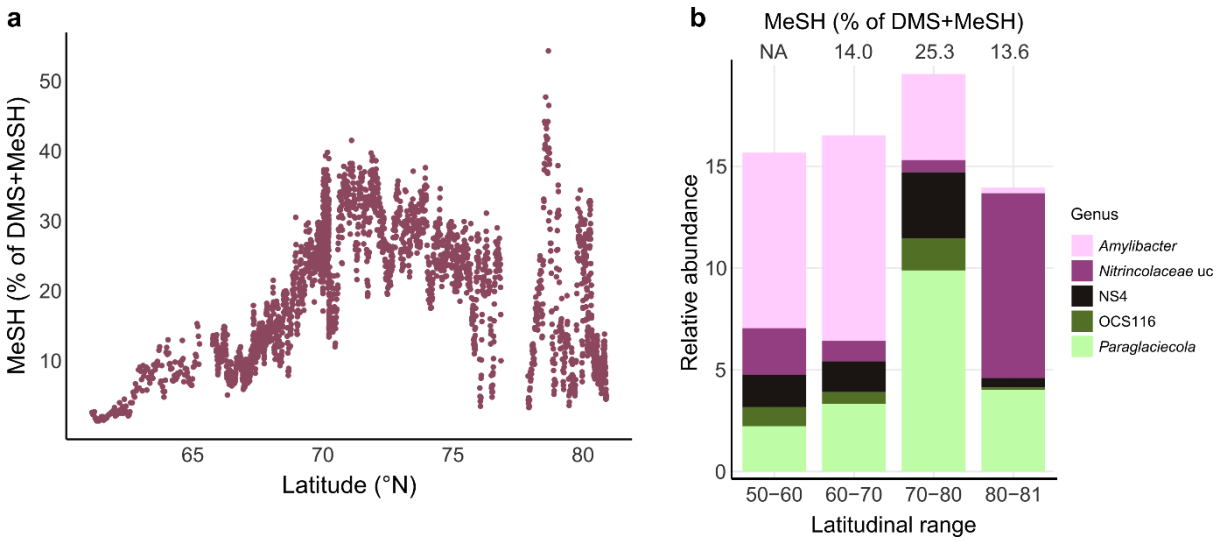

Fig 5a: Latitudinal variation of the MeSH fraction to the total sulphur compounds measured (DMS+MeSH), Fig. 5b: Relative abundance of selected bacterial genera by latitudinal range and associated MeSH/DMS ratio. NA: not available; uc: unclassified.

5 Conclusion

We present the first measurements of DMS, MeSH and other trace gases along a transect from the North Atlantic to the ice-covered Arctic Ocean. High-resolution latitudinal data between 57°N and 80°N were complemented with vertical profiles at sea-ice stations >80°N. Whereas isoprene, acetone, acetaldehyde and acetonitrile concentrations decreased northwards, CO, DMS and MeSH were uncorrelated with latitude and retained considerable concentrations in polar waters. Hence, these probably have phytoplankton-driven origins with regional variability, e.g. through localized blooms and/or the presence of sea-ice. The DMS peak in polar waters likely corresponded to sea ice as reservoir of DMS (Levasseur, 2013) and the prevalence of DMS-emitting phytoplankton. The marked correlation between DMS and Chl a in the diatom-dominated region >80°N represent a typical marginal sea ice zone effect. The missing correlation between DMS and MeSH suggested different processes of production and degradation, although they both originate from DMSP. Although DMS was overall more abundant, MeSH contributed on average 20% (and up to 50%) to the total DMS+MeSH budget, advising to consider MeSH as secondary aerosol producer in some regions. The potential importance of MeSH was underlined by more and stronger bacterial correlations than DMS, indicating that microbiological DMSP demethylation is important across extensive latitudinal gradients. Notably, higher acetaldehyde concentrations >80°N suggests that ice-covered regions could be a reservoir of acetaldehyde. While artefacts from off-line measurements (sampling through Niskin bottles) cannot be completely excluded, this result indicates a potential role of this reactive compound in regional atmospheric chemistry. To further investigate marine trace gas dynamics, including the rapidly changing Arctic, further measurements in the different reservoirs (ocean, atmosphere, ice) are necessary. In conclusion, the shown patterns in trace gas concentrations in high spatial resolution provide important insights into climatically and biologically relevant compounds and their connection to microbiology.

References

Alvarez, L. A., Exton, D. A., Timmis, K. N., Suggett, D. J., and McGenity, T. J.: Characterization of marine isoprene-degrading communities, Environmental Microbiology, 11, 3280–3291, https://doi.org/10.1111/j.1462-2920.2009.02069.x, 2009.

von Appen, W.-J., Waite, A. M., Bergmann, M., Bienhold, C., Boebel, O., Bracher, A., Cisewski, B., Hagemann, J., Hoppema, M., Iversen, M. H., Konrad, C., Krumpen, T., Lochthofen, N., Metfies, K., Niehoff, B., Nöthig, E.-M., Purser, A., Salter, I., Schaber, M., Scholz, D., Soltwedel, T., Torres-Valdes, S., Wekerle, C., Wenzhöfer, F., Wietz, M., and Boetius, A.: Sea-ice derived meltwater stratification slows the biological carbon pump: results from continuous observations, Nat Commun, 12, 7309, https://doi.org/10.1038/s41467-021-26943-z, 2021.

Arrigo, K. R. and van Dijken, G. L.: Continued increases in Arctic Ocean primary production, Progress in Oceanography, 136, 60–70, https://doi.org/10.1016/j.pocean.2015.05.002, 2015.

Assmy, P., Fernández-Méndez, M., Duarte, P., Meyer, A., Randelhoff, A., Mundy, C. J., Olsen, L. M., Kauko, H. M., Bailey, A., Chierici, M., Cohen, L., Doulgeris, A. P., Ehn, J. K., Fransson, A., Gerland, S., Hop, H., Hudson, S. R., Hughes, N., Itkin, P., Johnsen, G., King, J. A., Koch, B. P., Koenig, Z., Kwasniewski, S., Laney, S. R., Nicolaus, M., Pavlov, A. K., Polashenski, C. M., Provost, C., Rösel, A., Sandbu, M., Spreen, G., Smedsrud, L. H., Sundfjord, A., Taskjelle, T., Tatarek, A., Wiktor, J., Wagner, P. M., Wold, A., Steen, H., and Granskog, M. A.: Leads in Arctic pack ice enable early phytoplankton blooms below snow-covered sea ice, Sci Rep, 7, 40850, https://doi.org/10.1038/srep40850, 2017.

Baudic, A., Gros, V., Sauvage, S., Locoge, N., Sanchez, O., Sarda-Estève, R., Kalogridis, C., Petit, J.-E., Bonnaire, N., Baisnée, D., Favez, O., Albinet, A., Sciare, J., and Bonsang, B.: Seasonal variability and source apportionment of volatile organic compounds (VOCs) in the Paris megacity (France), Atmos. Chem. Phys., 16, 11961–11989, https://doi.org/10.5194/acp-16-11961-2016, 2016.

Beale, R., Dixon, J. L., Arnold, S. R., Liss, P. S., and Nightingale, P. D.: Methanol, acetaldehyde, and acetone in the surface waters of the Atlantic Ocean: OVOCs in The Atlantic Ocean, J. Geophys. Res. Oceans, 118, 5412–5425, https://doi.org/10.1002/jgrc.20322, 2013.

Bikkina, S., Kawamura, K., Miyazaki, Y., and Fu, P.: High abundances of oxalic, azelaic, and glyoxylic acids and methylglyoxal in the open ocean with high biological activity: Implication for secondary OA formation from isoprene: Oceanic control on atmospheric SOA, Geophys. Res. Lett., 41, 3649–3657, https://doi.org/10.1002/2014GL059913, 2014.

Blake, R. S., Monks, P. S., and Ellis, A. M.: Proton-Transfer Reaction Mass Spectrometry, Chem. Rev., 109, 861–896, https://doi.org/10.1021/cr800364q, 2009.

Bonsang, B., Polle, C., and Lambert, G.: Evidence for marine production of isoprene, Geophys. Res. Lett., 19, 1129–1132, https://doi.org/10.1029/92GL00083, 1992.

Bonsang, B., Gros, V., Peeken, I., Yassaa, N., Bluhm, K., Zoellner, E., Sarda-Esteve, R., and Williams, J.: Isoprene emission from phytoplankton monocultures: the relationship with chlorophyll-a, cell volume and carbon content, Environ. Chem., 7, 554, https://doi.org/10.1071/EN09156, 2010.

Butkovskaya, N. I. and Setser, D. W.: Product Branching Fractions and Kinetic Isotope Effects for the Reactions of OH and OD Radicals with CH_3SH and CH_3SD, J. Phys. Chem. A, 103, 6921–6929, https://doi.org/10.1021/jp9914828, 1999.

Callahan, B. J., McMurdie, P. J., Rosen, M. J., Han, A. W., Johnson, A. J. A., and Holmes, S. P.: DADA2: High-resolution sample inference from Illumina amplicon data, Nat Methods, 13, 581–583, https://doi.org/10.1038/nmeth.3869, 2016.

Campen, H. I., Arévalo-Martínez, D. L., Artioli, Y., Brown, I. J., Kitidis, V., Lessin, G., Rees, A. P., and Bange, H. W.: The role of a changing Arctic Ocean and climate for the biogeochemical cycling of dimethyl sulphide and carbon monoxide, Ambio, 51, 411–422, https://doi.org/10.1007/s13280-021-01612-z, 2022.

Carrión, O., McGenity, T. J., and Murrell, J. C.: Molecular Ecology of Isoprene-Degrading Bacteria, Microorganisms, 8, 967, https://doi.org/10.3390/microorganisms8070967, 2020.

Charlson, R. J., Lovelock, J. E., Andreae, M. O., and Warren, S. G.: Oceanic phytoplankton, atmospheric sulphur, cloud albedo and climate, Nature, 326, 655–661, https://doi.org/10.1038/326655a0, 1987.

Ciuraru, R., Fine, L., Pinxteren, M. van, D'Anna, B., Herrmann, H., and George, C.: Unravelling New Processes at Interfaces: Photochemical Isoprene Production at the Sea Surface, Environ. Sci. Technol., 49, 13199–13205, https://doi.org/10.1021/acs.est.5b02388, 2015.

Conte, L., Szopa, S., Séférian, R., and Bopp, L.: The oceanic cycle of carbon monoxide and its emissions to the atmosphere, Biogeosciences, 16, 881–902, https://doi.org/10.5194/bg-16-881-2019, 2019.

Curson, A. R. J., Todd, J. D., Sullivan, M. J., and Johnston, A. W. B.: Catabolism of dimethylsulphoniopropionate: microorganisms, enzymes and genes, Nat Rev Microbiol, 9, 849–859, https://doi.org/10.1038/nrmicro2653, 2011.

Davie-Martin, C. L., Giovannoni, S. J., Behrenfeld, M. J., Penta, W. B., and Halsey, K. H.: Seasonal and Spatial Variability in the Biogenic Production and Consumption of Volatile Organic Compounds (VOCs) by Marine Plankton in the North Atlantic Ocean, Front. Mar. Sci., 7, 611870, https://doi.org/10.3389/fmars.2020.611870, 2020.

Degerlund, M. and Eilertsen, H. C.: Main Species Characteristics of Phytoplankton Spring Blooms in NE Atlantic and Arctic Waters (68–80° N), Estuaries and Coasts, 33, 242–269, https://doi.org/10.1007/s12237-009-9167-7, 2010.

Duncan, B. N., Logan, J. A., Bey, I., Megretskaia, I. A., Yantosca, R. M., Novelli, P. C., Jones, N. B., and Rinsland, C. P.: Global budget of CO, 1988–1997: Source estimates and validation with a global model, J. Geophys. Res., 112, D22301, https://doi.org/10.1029/2007JD008459, 2007.

Dybwad, C., Assmy, P., Olsen, L. M., Peeken, I., Nikolopoulos, A., Krumpen, T., Randelhoff, A., Tatarek, A., Wiktor, J. M., and Reigstad, M.: Carbon Export in the Seasonal Sea Ice Zone North of Svalbard From Winter to Late Summer, Front. Mar. Sci., 7, 525800, https://doi.org/10.3389/fmars.2020.525800, 2021.

Fernández-Méndez, M., Wenzhöfer, F., Peeken, I., Sørensen, H. L., Glud, R. N., and Boetius, A.: Composition, Buoyancy Regulation and Fate of Ice Algal Aggregates in the Central Arctic Ocean, PLoS ONE, 9, e107452, https://doi.org/10.1371/journal.pone.0107452, 2014.

Fichot, C. G. and Miller, W. L.: An approach to quantify depth-resolved marine photochemical fluxes using remote sensing: Application to carbon monoxide (CO) photoproduction, Remote Sensing of Environment, 114, 1363–1377, https://doi.org/10.1016/j.rse.2010.01.019, 2010.

Fischer, E. V., Jacob, D. J., Millet, D. B., Yantosca, R. M., and Mao, J.: The role of the ocean in the global atmospheric budget of acetone: ATMOSPHERIC BUDGET OF ACETONE, Geophys. Res. Lett., 39, n/a-n/a, https://doi.org/10.1029/2011GL050086, 2012.

Galí, M. and Simó, R.: Occurrence and cycling of dimethylated sulfur compounds in the Arctic during summer receding of the ice edge, Marine Chemistry, 122, 105–117, https://doi.org/10.1016/j.marchem.2010.07.003, 2010.

Galí, M., Lizotte, M., Kieber, D. J., Randelhoff, A., Hussherr, R., Xue, L., Dinasquet, J., Babin, M., Rehm, E., and Levasseur, M.: DMS emissions from the Arctic marginal ice zone, Elementa: Science of the Anthropocene, 9, 00113, https://doi.org/10.1525/elementa.2020.00113, 2021.

Galindo, V., Levasseur, M., Mundy, C. J., Gosselin, M., Tremblay, J.-É., Scarratt, M., Gratton, Y., Papakiriakou, T., Poulin, M., and Lizotte, M.: Biological and physical processes influencing sea ice, under-ice algae, and dimethylsulfoniopropionate during spring in the Canadian Arctic Archipelago, J. Geophys. Res. Oceans, 119, 3746–3766, https://doi.org/10.1002/2013JC009497, 2014.

GEBCO Bathymetric Compilation Group 2022: The GEBCO_2022 Grid - a continuous terrain model of the global oceans and land., https://doi.org/10.5285/E0F0BB80-AB44-2739-E053-6C86ABC0289C, 2022.

Gonçalves-Araujo, R., Rabe, B., Peeken, I., and Bracher, A.: High colored dissolved organic matter (CDOM) absorption in surface waters of the central-eastern Arctic Ocean: Implications for biogeochemistry and ocean color algorithms, PLoS ONE, 13, e0190838, https://doi.org/10.1371/journal.pone.0190838, 2018.

de Gouw, J. and Warneke, C.: Measurements of volatile organic compounds in the earth's atmosphere using proton-transfer-reaction mass spectrometry, Mass Spectrom. Rev., 26, 223–257, https://doi.org/10.1002/mas.20119, 2007.

Gros, V., Bonsang, B., and Sarda Esteve, R.: Atmospheric carbon monoxide 'in situ' monitoring by automatic gas chromatography, Chemosphere - Global Change Science, 1, 153–161, https://doi.org/10.1016/S1465-9972(99)00010-0, 1999.

Gros, V., Peeken, I., Bluhm, K., Zöllner, E., Sarda-Esteve, R., and Bonsang, B.: Carbon monoxide emissions by phytoplankton: evidence from laboratory experiments, Environ. Chem., 6, 369, https://doi.org/10.1071/EN09020, 2009.

Guenther, A., Hewitt, C. N., Erickson, D., Fall, R., Geron, C., Graedel, T., Harley, P., Klinger, L., Lerdau, M., Mckay, W. A., Pierce, T., Scholes, B., Steinbrecher, R., Tallamraju, R., Taylor, J., and Zimmerman, P.: A global model of natural volatile organic compound emissions, J. Geophys. Res., 100, 8873, https://doi.org/10.1029/94JD02950, 1995.

Hackenberg, S. C., Andrews, S. J., Airs, R., Arnold, S. R., Bouman, H. A., Brewin, R. J. W., Chance, R. J., Cummings, D., Dall'Olmo, G., Lewis, A. C., Minaeian, J. K., Reifel, K. M., Small, A., Tarran, G. A., Tilstone, G. H., and Carpenter, L. J.: Potential controls of isoprene in the surface ocean: Isoprene Controls in the Surface Ocean, Global Biogeochem. Cycles, 31, 644–662, https://doi.org/10.1002/2016GB005531, 2017.

Hayashida, H., Carnat, G., Galí, M., Monahan, A. H., Mortenson, E., Sou, T., and Steiner, N. S.: Spatiotemporal Variability in Modeled Bottom Ice and Sea Surface Dimethylsulfide Concentrations and Fluxes in the Arctic During 1979–2015, Global Biogeochem. Cycles, 34, https://doi.org/10.1029/2019GB006456, 2020.

Hegseth, E. N. and Sundfjord, A.: Intrusion and blooming of Atlantic phytoplankton species in the high Arctic, Journal of Marine Systems, 74, 108–119, https://doi.org/10.1016/j.jmarsys.2007.11.011, 2008.

Jackson, R. and Gabric, A.: Climate Change Impacts on the Marine Cycling of Biogenic Sulfur: A Review, Microorganisms, 10, 1581, https://doi.org/10.3390/microorganisms10081581, 2022.

Jacob, D. J., Field, B. D., Jin, E. M., Bey, I., Li, Q., Logan, J. A., Yantosca, R. M., and Singh, H. B.: Atmospheric budget of acetone: ATMOSPHERIC BUDGET OF ACETONE, J. Geophys. Res., 107, ACH 5-1-ACH 5-17, https://doi.org/10.1029/2001JD000694, 2002.

Jarníková, T., Dacey, J., Lizotte, M., Levasseur, M., and Tortell, P.: The distribution of methylated sulfur compounds, DMS and DMSP, in Canadian subarctic and Arctic marine waters during summer 2015, Biogeosciences, 15, 2449–2465, https://doi.org/10.5194/bg-15-2449-2018, 2018.

Kameyama, S., Tanimoto, H., Inomata, S., Tsunogai, U., Ooki, A., Takeda, S., Obata, H., Tsuda, A., and Uematsu, M.: High-resolution measurement of multiple volatile organic compounds dissolved in seawater using equilibrator inlet–proton transfer reaction-mass spectrometry (EI–PTR-MS), Marine Chemistry, 122, 59–73, https://doi.org/10.1016/j.marchem.2010.08.003, 2010.

Kansal, A.: Sources and reactivity of NMHCs and VOCs in the atmosphere: A review, Journal of Hazardous Materials, 166, 17–26, https://doi.org/10.1016/j.jhazmat.2008.11.048, 2009.

Kettle, A. J., Rhee, T. S., von Hobe, M., Poulton, A., Aiken, J., and Andreae, M. O.: Assessing the flux of different volatile sulfur gases from the ocean to the atmosphere, J. Geophys. Res., 106, 12193–12209, https://doi.org/10.1029/2000JD900630, 2001.

Kiene, R. P.: Production of methanethiol from dimethylsulfoniopropionate in marine surface waters, Marine Chemistry, 54, 69–83, https://doi.org/10.1016/0304-4203(96)00006-0, 1996.

Kiene, R. P. and Linn, L. J.: The fate of dissolved dimethylsulfoniopropionate (DMSP) in seawater: tracer studies using 35S-DMSP, Geochimica et Cosmochimica Acta, 64, 2797–2810, https://doi.org/10.1016/S0016-7037(00)00399-9, 2000.

Kiene, R. P., Willams T.E., Esson, K., Tortell, P., and Dacey, J.W. H.: Concentrations and Sea-Air Fluxes in the Subarctic NE Pacific Ocean, AGU, Fall Meeting, San Francisco, 2017.

Kilgour, D. B., Novak, G. A., Sauer, J. S., Moore, A. N., Dinasquet, J., Amiri, S., Franklin, E. B., Mayer, K., Winter, M., Morris, C. K., Price, T., Malfatti, F., Crocker, D. R., Lee, C., Cappa, C. D., Goldstein, A. H., Prather, K. A., and Bertram, T. H.: Marine gas-phase sulfur emissions during an induced phytoplankton bloom, Atmos. Chem. Phys., 22, 1601–1613, https://doi.org/10.5194/acp-22-1601-2022, 2022.

Lana, A., Simó, R., Vallina, S. M., and Dachs, J.: Re-examination of global emerging patterns of ocean DMS concentration, Biogeochemistry, 110, 173–182, https://doi.org/10.1007/s10533-011-9677-9, 2012.

Landa, M., Burns, A. S., Durham, B. P., Esson, K., Nowinski, B., Sharma, S., Vorobev, A., Nielsen, T., Kiene, R. P., and Moran, M. A.: Sulfur metabolites that facilitate oceanic phytoplankton–bacteria carbon flux, ISME J, 13, 2536–2550, https://doi.org/10.1038/s41396-019-0455-3, 2019.

Lannuzel, D., Tedesco, L., van Leeuwe, M., Campbell, K., Flores, H., Delille, B., Miller, L., Stefels, J., Assmy, P., Bowman, J., Brown, K., Castellani, G., Chierici, M., Crabeck, O., Damm, E., Else, B., Fransson, A., Fripiat, F., Geilfus, N.-X., Jacques, C., Jones, E., Kaartokallio, H., Kotovitch, M., Meiners, K., Moreau, S., Nomura, D., Peeken, I., Rintala, J.-M., Steiner, N., Tison, J.-L., Vancoppenolle, M., Van der Linden, F., Vichi, M., and Wongpan, P.: The future of Arctic sea-ice biogeochemistry and ice-associated ecosystems, Nat. Clim. Chang., 10, 983–992, https://doi.org/10.1038/s41558-020-00940-4, 2020.

Lawson, S. J., Law, C. S., Harvey, M. J., Bell, T. G., Walker, C. F., de Bruyn, W. J., and Saltzman, E. S.: Methanethiol, dimethyl sulfide and acetone over biologically productive waters in the southwest Pacific Ocean, Atmos. Chem. Phys., 20, 3061–3078, https://doi.org/10.5194/acp-20-3061-2020, 2020.

Leck, C. and Rodhe, H.: Emissions of marine biogenic sulfur to the atmosphere of northern Europe, J Atmos Chem, 12, 63–86, https://doi.org/10.1007/BF00053934, 1991.

Levasseur, M.: Impact of Arctic meltdown on the microbial cycling of sulphur, Nature Geosci, 6, 691–700, https://doi.org/10.1038/ngeo1910, 2013.

Lindinger, W. and Jordan, A.: Proton-transfer-reaction mass spectrometry (PTR–MS): on-line monitoring of volatile organic compounds at pptv levels, Chem. Soc. Rev., 27, 347, https://doi.org/10.1039/a827347z, 1998.

Liu, J., Liu, J., Zhang, S.-H., Liang, J., Lin, H., Song, D., Yang, G.-P., Todd, J. D., and Zhang, X.-H.: Novel Insights Into Bacterial Dimethylsulfoniopropionate Catabolism in the East China Sea, Front. Microbiol., 9, 3206, https://doi.org/10.3389/fmicb.2018.03206, 2018.

Love, C. R., Arrington, E. C., Gosselin, K. M., Reddy, C. M., Van Mooy, B. A. S., Nelson, R. K., and Valentine, D. L.: Microbial production and consumption of hydrocarbons in the global ocean, Nat Microbiol, 6, 489–498, https://doi.org/10.1038/s41564-020-00859-8, 2021.

Marandino, C. A.: Oceanic uptake and the global atmospheric acetone budget, Geophys. Res. Lett., 32, L15806, https://doi.org/10.1029/2005GL023285, 2005.

Martin, M.: Cutadapt removes adapter sequences from high-throughput sequencing reads, EMBnet j., 17, 10, https://doi.org/10.14806/ej.17.1.200, 2011.

Massicotte, P., Peeken, I., Katlein, C., Flores, H., Huot, Y., Castellani, G., Arndt, S., Lange, B. A., Tremblay, J., and Babin, M.: Sensitivity of Phytoplankton Primary Production Estimates to Available Irradiance Under Heterogeneous Sea Ice Conditions, J. Geophys. Res. Oceans, 124, 5436–5450, https://doi.org/10.1029/2019JC015007, 2019.

Metfies, K., Schroeder, F., Hessel, J., Wollschläger, J., Micheller, S., Wolf, C., Kilias, E., Sprong, P., Neuhaus, S., Frickenhaus, S., and Petersen, W.: High-resolution monitoring of marine protists based on an observation strategy integrating automated on-board filtration and molecular analyses, Ocean Sci., 12, 1237–1247, https://doi.org/10.5194/os-12-1237-2016, 2016.

Metfies, K., Hessel, J., Klenk, R., Petersen, W., Wiltshire, K. H., and Kraberg, A.: Uncovering the intricacies of microbial community dynamics at Helgoland Roads at the end of a spring bloom using automated sampling and 18S meta-barcoding, PLoS ONE, 15, e0233921, https://doi.org/10.1371/journal.pone.0233921, 2020.

Moran, M. A. and Durham, B. P.: Sulfur metabolites in the pelagic ocean, Nat Rev Microbiol, 17, 665–678, https://doi.org/10.1038/s41579-019-0250-1, 2019.

Moran, M. A., Reisch, C. R., Kiene, R. P., and Whitman, W. B.: Genomic Insights into Bacterial DMSP Transformations, Annu. Rev. Mar. Sci., 4, 523–542, https://doi.org/10.1146/annurev-marine-120710-100827, 2012.

Morel, A. and Gentili, B.: A simple band ratio technique to quantify the colored dissolved and detrital organic material from ocean color remotely sensed data, Remote Sensing of Environment, 113, 998–1011, https://doi.org/10.1016/j.rse.2009.01.008, 2009.

Mungall, E. L., Croft, B., Lizotte, M., Thomas, J. L., Murphy, J. G., Levasseur, M., Martin, R. V., Wentzell, J. J. B., Liggio, J., and Abbatt, J. P. D.: Dimethyl sulfide in the summertime Arctic atmosphere: measurements and source sensitivity simulations, Atmos. Chem. Phys., 16, 6665–6680, https://doi.org/10.5194/acp-16-6665-2016, 2016.

Nikolopoulos, Anna, Janout, Markus A, Hölemann, Jens A, Juhls, Bennet, Korhonen, Meri, and Randelhoff, Achim: Physical oceanography measured on water bottle samples during POLARSTERN cruise PS92 (ARK-XXIX/1), https://doi.org/10.1594/PANGAEA.861866, 2016.

Nöthig, E.-M., Bracher, A., Engel, A., Metfies, K., Niehoff, B., Peeken, I., Bauerfeind, E., Cherkasheva, A., Gäbler-Schwarz, S., Hardge, K., Kilias, E., Kraft, A., Mebrahtom Kidane, Y., Lalande, C., Piontek, J., Thomisch, K., and Wurst, M.: Summertime plankton ecology in Fram Strait—a compilation of long- and short-term observations, Polar Research, 34, 23349, https://doi.org/10.3402/polar.v34.23349, 2015.

Novak, G. A., Kilgour, D. B., Jernigan, C. M., Vermeuel, M. P., and Bertram, T. H.: Oceanic emissions of dimethyl sulfide and methanethiol and their contribution to sulfur dioxide production in the marine atmosphere, Atmos. Chem. Phys., 22, 6309–6325, https://doi.org/10.5194/acp-22-6309-2022, 2022.

Nowinski, B., Motard-Côté, J., Landa, M., Preston, C. M., Scholin, C. A., Birch, J. M., Kiene, R. P., and Moran, M. A.: Microdiversity and temporal dynamics of marine bacterial dimethylsulfoniopropionate genes, Environ Microbiol, 21, 1687–1701, https://doi.org/10.1111/1462-2920.14560, 2019.

Ooki, A., Nomura, D., Nishino, S., Kikuchi, T., and Yokouchi, Y.: A global-scale map of isoprene and volatile organic iodine in surface seawater of the A rctic, N orthwest P acific, I ndian, and S outhern O ceans, J. Geophys. Res. Oceans, 120, 4108–4128, https://doi.org/10.1002/2014JC010519, 2015.

Oziel, L., Baudena, A., Ardyna, M., Massicotte, P., Randelhoff, A., Sallée, J.-B., Ingvaldsen, R. B., Devred, E., and Babin, M.: Faster Atlantic currents drive poleward expansion of temperate phytoplankton in the Arctic Ocean, Nat Commun, 11, 1705, https://doi.org/10.1038/s41467-020-15485-5, 2020.

Parada, A. E., Needham, D. M., and Fuhrman, J. A.: Every base matters: assessing small subunit rRNA primers for marine microbiomes with mock communities, time series and global field samples: Primers for marine microbiome studies, Environ Microbiol, 18, 1403–1414, https://doi.org/10.1111/1462-2920.13023, 2016.

Park, K.-T., Lee, K., Yoon, Y.-J., Lee, H.-W., Kim, H.-C., Lee, B.-Y., Hermansen, O., Kim, T.-W., and Holmén, K.: Linking atmospheric dimethyl sulfide and the Arctic Ocean spring bloom: ATMOSPHERIC DMS IN THE ARCTIC SPRING BLOOM, Geophys. Res. Lett., 40, 155–160, https://doi.org/10.1029/2012GL054560, 2013.

Peeken, I.: The Expedition PS92 of the Research Vessel Polarstern to the Arctic Ocean in 2015, Alfred-Wegener-Institut, Helmholtz-Zentrum für Polar- und Meeresforschung, https://doi.org/10.2312/BZPM_0694_2016, 2016.

Petersen, W.: FerryBox systems: State-of-the-art in Europe and future development, Journal of Marine Systems, 140, 4–12, https://doi.org/10.1016/j.jmarsys.2014.07.003, 2014.

Phillips, D. P., Hopkins, F. E., Bell, T. G., Liss, P. S., Nightingale, P. D., Reeves, C. E., Wohl, C., and Yang, M.: Air–sea exchange of acetone, acetaldehyde, DMS and isoprene at a UK coastal site, Atmos. Chem. Phys., 21, 10111–10132, https://doi.org/10.5194/acp-21-10111-2021, 2021.

Polyakov, I. V., Alkire, M. B., Bluhm, B. A., Brown, K. A., Carmack, E. C., Chierici, M., Danielson, S. L., Ellingsen, I., Ershova, E. A., Gårdfeldt, K., Ingvaldsen, R. B., Pnyushkov, A. V., Slagstad, D., and Wassmann, P.: Borealization of the Arctic Ocean in Response to Anomalous Advection From Sub-Arctic Seas, Front. Mar. Sci., 7, 491, https://doi.org/10.3389/fmars.2020.00491, 2020.

Quast, C., Pruesse, E., Yilmaz, P., Gerken, J., Schweer, T., Yarza, P., Peplies, J., and Glöckner, F. O.: The SILVA ribosomal RNA gene database project: improved data processing and web-based tools, Nucleic Acids Research, 41, D590–D596, https://doi.org/10.1093/nar/gks1219, 2012.

Rodríguez-Ros, P., Cortés, P., Robinson, C. M., Nunes, S., Hassler, C., Royer, S.-J., Estrada, M., Sala, M. M., and Simó, R.: Distribution and Drivers of Marine Isoprene Concentration across the Southern Ocean, Atmosphere, 11, 556, https://doi.org/10.3390/atmos11060556, 2020.

Schmale, J., Zieger, P., and Ekman, A. M. L.: Aerosols in current and future Arctic climate, Nat. Clim. Chang., 11, 95–105, https://doi.org/10.1038/s41558-020-00969-5, 2021.

Shaw, G. E.: Bio-controlled thermostasis involving the sulfur cycle, Climatic Change, 5, 297–303, https://doi.org/10.1007/BF02423524, 1983.

Shaw, S. L., Gantt, B., and Meskhidze, N.: Production and Emissions of Marine Isoprene and Monoterpenes: A Review, Advances in Meteorology, 2010, 1–24, https://doi.org/10.1155/2010/408696, 2010.

Simó, R., Cortés-Greus, P., Rodríguez-Ros, P., and Masdeu-Navarro, M.: Substantial loss of isoprene in the surface ocean due to chemical and biological consumption, Commun Earth Environ, 3, 20, https://doi.org/10.1038/s43247-022-00352-6, 2022.

Singh, H. B.: Analysis of the atmospheric distribution, sources, and sinks of oxygenated volatile organic chemicals based on measurements over the Pacific during TRACE-P, J. Geophys. Res., 109, D15S07, https://doi.org/10.1029/2003JD003883, 2004.

Song, G., Xie, H., Aubry, C., Zhang, Y., Gosselin, M., Mundy, C. J., Philippe, B., and Papakyriakou, T. N.: Spatiotemporal variations of dissolved organic carbon and carbon monoxide in first-year sea ice in the western Canadian Arctic, J. Geophys. Res., 116, C00G05, https://doi.org/10.1029/2010JC006867, 2011.

Stefels, J., Steinke, M., Turner, S., Malin, G., and Belviso, S.: Environmental constraints on the production and removal of the climatically active gas dimethylsulphide (DMS) and implications for ecosystem modelling, Biogeochemistry, 83, 245–275, https://doi.org/10.1007/s10533-007-9091-5, 2007.

Sun, J., Todd, J. D., Thrash, J. C., Qian, Y., Qian, M. C., Temperton, B., Guo, J., Fowler, E. K., Aldrich, J. T., Nicora, C. D., Lipton, M. S., Smith, R. D., De Leenheer, P., Payne, S. H., Johnston, A. W. B., Davie-Martin, C. L., Halsey, K. H., and Giovannoni, S. J.: The abundant marine bacterium Pelagibacter simultaneously catabolizes dimethylsulfoniopropionate to the gases dimethyl sulfide and methanethiol, Nat Microbiol, 1, 16065, https://doi.org/10.1038/nmicrobiol.2016.65, 2016.

Sunagawa, S., Coelho, L. P., Chaffron, S., Kultima, J. R., Labadie, K., Salazar, G., Djahanschiri, B., Zeller, G., Mende, D. R., Alberti, A., Cornejo-Castillo, F. M., Costea, P. I., Cruaud, C., d'Ovidio, F., Engelen, S., Ferrera, I., Gasol, J. M., Guidi, L., Hildebrand, F., Kokoszka, F., Lepoivre, C., Lima-Mendez, G., Poulain, J., Poulos, B. T., Royo-Llonch, M., Sarmento, H., Vieira-Silva, S., Dimier, C., Picheral, M., Searson, S., Kandels-Lewis, S., Tara Oceans coordinators, Bowler, C., de Vargas, C., Gorsky, G., Grimsley, N., Hingamp, P., Iudicone, D., Jaillon, O., Not, F., Ogata, H., Pesant, S., Speich, S., Stemmann, L., Sullivan, M. B., Weissenbach, J., Wincker, P., Karsenti, E., Raes, J., Acinas, S. G., Bork, P., Boss, E., Bowler, C., Follows, M., Karp-Boss, L., Krzic, U., Reynaud, E. G., Sardet, C., Sieracki, M., and Velayoudon, D.: Structure and function of the global ocean microbiome, Science, 348, 1261359, https://doi.org/10.1126/science.1261359, 2015.

Tanimoto, H., Kameyama, S., Omori, Y., Inomata, S., and Tsunogai, U.: High-Resolution Measurement of Volatile Organic Compounds Dissolved in Seawater Using Equilibrator Inlet-Proton Transfer Reaction-Mass Spectrometry (EI-PTR-MS), in: Western Pacific Air-Sea Interaction Study, edited by: Uematsu, M., Yokouchi, Y., Watanabe, Y., Takeda, S., and Yamanaka, Y., TERRAPUB, 89–115, https://doi.org/10.5047/w-pass.a02.001, 2014.

Thompson, H. F., Summers, S., Yuecel, R., and Gutierrez, T.: Hydrocarbon-Degrading Bacteria Found Tightly Associated with the 50–70 μm Cell-Size Population of Eukaryotic Phytoplankton in Surface Waters of a Northeast Atlantic Region, Microorganisms, 8, 1955, https://doi.org/10.3390/microorganisms8121955, 2020.

Tison, J.-L., Brabant, F., Dumont, I., and Stefels, J.: High-resolution dimethyl sulfide and dimethylsulfoniopropionate time series profiles in decaying summer first-year sea ice at Ice Station Polarstern, western Weddell Sea, Antarctica, J. Geophys. Res., 115, G04044, https://doi.org/10.1029/2010JG001427, 2010.

Tolli, J. D. and Taylor, C. D.: Biological CO oxidation in the Sargasso Sea and in Vineyard Sound, Massachusetts, Limnol. Oceanogr., 50, 1205–1212, https://doi.org/10.4319/lo.2005.50.4.1205, 2005.

Tran, S., Bonsang, B., Gros, V., Peeken, I., Sarda-Esteve, R., Bernhardt, A., and Belviso, S.: A survey of carbon monoxide and non-methane hydrocarbons in the Arctic Ocean during summer 2010, Biogeosciences, 10, 1909–1935, https://doi.org/10.5194/bg-10-1909-2013, 2013.

Tyndall, G. S. and Ravishankara, A. R.: Atmospheric oxidation of reduced sulfur species, Int. J. Chem. Kinet., 23, 483–527, https://doi.org/10.1002/kin.550230604, 1991.

Uhlig, C., Damm, E., Peeken, I., Krumpen, T., Rabe, B., Korhonen, M., and Ludwichowski, K.-U.: Sea Ice and Water Mass Influence Dimethylsulfide Concentrations in the Central Arctic Ocean, Front. Earth Sci., 7, 179, https://doi.org/10.3389/feart.2019.00179, 2019.

Wang, S., Hornbrook, R. S., Hills, A., Emmons, L. K., Tilmes, S., Lamarque, J., Jimenez, J. L., Campuzano-Jost, P., Nault, B. A., Crounse, J. D., Wennberg, P. O., Kim, M., Allen, H., Ryerson, T. B., Thompson, C. R., Peischl, J., Moore, F., Nance, D., Hall, B., Elkins, J., Tanner, D., Huey, L. G., Hall, S. R., Ullmann, K., Orlando, J. J., Tyndall, G. S., Flocke, F. M., Ray, E., Hanisco, T. F., Wolfe, G. M., St. Clair, J., Commane, R., Daube, B., Barletta, B., Blake, D. R., Weinzierl, B., Dollner, M., Conley, A., Vitt, F., Wofsy, S. C., Riemer, D. D., and Apel, E. C.: Atmospheric Acetaldehyde: Importance of Air-Sea Exchange and a Missing Source in the Remote Troposphere, Geophys. Res. Lett., 46, 5601–5613, https://doi.org/10.1029/2019GL082034, 2019.

Williams, J., Holzinger, R., Gros, V., Xu, X., Atlas, E., and Wallace, D. W. R.: Measurements of organic species in air and seawater from the tropical Atlantic: ORGANIC SPECIES IN AIR AND SEA, Geophys. Res. Lett., 31, https://doi.org/10.1029/2004GL020012, 2004.

Wilson, D. F., Swinnerton, J. W., and Lamontagne, R. A.: Production of Carbon Monoxide and Gaseous Hydrocarbons in Seawater: Relation to Dissolved Organic Carbon, Science, 168, 1577–1579, https://doi.org/10.1126/science.168.3939.1577, 1970.

Wohl, C., Capelle, D., Jones, A., Sturges, W. T., Nightingale, P. D., Else, B. G. T., and Yang, M.: Segmented flow coil equilibrator coupled to a proton-transfer-reaction mass spectrometer for measurements of a broad range of volatile organic compounds in seawater, Ocean Sci., 15, 925–940, https://doi.org/10.5194/os-15-925-2019, 2019.

Wohl, C., Brown, I., Kitidis, V., Jones, A. E., Sturges, W. T., Nightingale, P. D., and Yang, M.: Underway seawater and atmospheric measurements of volatile organic compounds in the Southern Ocean, Biogeosciences, 17, 2593–2619, https://doi.org/10.5194/bg-17-2593-2020, 2020.

Wohl, C., Jones, A. E., Sturges, W. T., Nightingale, P. D., Else, B., Butterworth, B. J., and Yang, M.: Sea ice concentration impacts dissolved organic gases in the Canadian Arctic, Biogeosciences, 19, 1021–1045, https://doi.org/10.5194/bg-19-1021-2022, 2022.

Wollenburg, J. E., Katlein, C., Nehrke, G., Nöthig, E.-M., Matthiessen, J., Wolf- Gladrow, D. A., Nikolopoulos, A., Gázquez-Sanchez, F., Rossmann, L., Assmy, P., Babin, M., Bruyant, F., Beaulieu, M., Dybwad, C., and Peeken, I.: Ballasting by cryogenic gypsum enhances carbon export in a Phaeocystis under-ice bloom, Sci Rep, 8, 7703, https://doi.org/10.1038/s41598-018-26016-0, 2018.

Xie, H. and Gosselin, M.: Photoproduction of carbon monoxide in first-year sea ice in Franklin Bay, southeastern Beaufort Sea: PHOTOPRODUCTION OF CO IN SEA ICE, Geophys. Res. Lett., 32, n/a-n/a, https://doi.org/10.1029/2005GL022803, 2005.

Xie, H. and Zafiriou, O. C.: Evidence for significant photochemical production of carbon monoxide by particles in coastal and oligotrophic marine waters, Geophys. Res. Lett., 36, L23606, https://doi.org/10.1029/2009GL041158, 2009.

Yang, M., Beale, R., Liss, P., Johnson, M., Blomquist, B., and Nightingale, P.: Air–sea fluxes of oxygenated volatile organic compounds across the Atlantic Ocean, Atmos. Chem. Phys., 14, 7499–7517, https://doi.org/10.5194/acp-14-7499-2014, 2014.

Yuan, B., Koss, A. R., Warneke, C., Coggon, M., Sekimoto, K., and de Gouw, J. A.: Proton-Transfer-Reaction Mass Spectrometry: Applications in Atmospheric Sciences, Chem. Rev., 117, 13187–13229, https://doi.org/10.1021/acs.chemrev.7b00325, 2017.

Zannoni, N., Gros, V., Lanza, M., Sarda, R., Bonsang, B., Kalogridis, C., Preunkert, S., Legrand, M., Jambert, C., Boissard, C., and Lathiere, J.: OH reactivity and concentrations of biogenic volatile organic compounds in a Mediterranean forest of downy oak trees, Atmos. Chem. Phys., 16, 1619–1636, https://doi.org/10.5194/acp-16-1619-2016, 2016.

Zhou, X. and Mopper, K.: Photochemical production of low-molecular-weight carbonyl compounds in seawater and surface microlayer and their air-sea exchange, Marine Chemistry, 56, 201–213, https://doi.org/10.1016/S0304-4203(96)00076-X, 1997.

Zhu, Y. and Kieber, D. J.: Concentrations and Photochemistry of Acetaldehyde, Glyoxal, and Methylglyoxal in the Northwest Atlantic Ocean, Environ. Sci. Technol., 53, 9512–9521, https://doi.org/10.1021/acs.est.9b01631, 2019.

790

Author contributions

VG, RSE, BB, and IP designed the study. BB, VG and RSE performed trace gas measurements prior to the campaign; VG and RSE performed trace gas measurements on-board. IP coordinated all TRANSSIZ work, supervised the biological sampling on-board and subsequent performed pigments analyses. AN coordinated the oceanographic sampling and water mass
795 classification. KM set up the AUTOFIM sampling system and supervised DNA extraction. MW performed bacterial community analyses. VG, BB, IP and MW wrote the manuscript. All co-authors have read and contributed to the manuscript.

Competing interests

The authors declare no competing interests.

800

Acknowledgments

We are thankful to the captain, crew and scientists from the TRANSSIZ expedition (ARK XXIX/1; PS92), carried out under grant number AWI_PS92_00. We thank Francois Truong for help with data processing, as well as Josephine Rapp and Halina Tegetmeyer for help with amplicon sequencing. IP, MW and KM are funded by the PoF IV program "Changing Earth -
805 Sustaining our Future" Topic 6.1 of the Helmholtz Association. The publication is part of the FRAM Observatory under EPIC number 56216. We acknowledge financial support from AWI, CNRS and CEA.